Development of H-Radical Reactive Infrared Laser Deposition for The Study of Metal Hydrides Epitaxial Films

Kota Munefusa[(1)], Erika Fukushi[(1)], Junya Tanaka[(1)], Takayuki Harada[(2)] and Hiroyuki Oguchi[(1)]

Abstract: In this study, we try to synthesize LiH epitaxial thin films by H-radical reactive infrared laser deposition. We demonstrate that efficient use of H-radical enables us to obtain highly pure and highly crystalline epitaxial films. We also demonstrate that the low energy infrared laser heating of the starting material is a key mechanism to prevent reactions between the film and substrate. In addition, we discuss orientation controllability and elemental substitution capability of our deposition method. In summary, this study verifies the high potential of H-radical reactive infrared laser deposition for the synthesis of metal hydride epitaxial films and development of their physical properties.

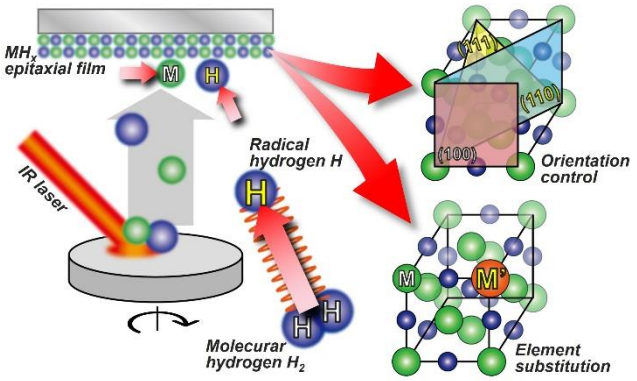

1. INTRODUCTION

Metal hydrides (MH_x) are compounds obtained by chemical bonding of metals and hydrogen [(1)]. Metal hydrides are attractive functional materials since those often exhibit unique functionalities that can only be realized with hydrogen-containing materials. Such special functionalities include, for example, hydrogen absorption and desorption [(2)], hydride ion conduction [(3)], and changes in translucency accompanied with the absorption and desorption of hydrogen [(4)]. Recently, high-temperature superconductivity has been reported [LaH_{10} [(5)], H_3S [(6)]], and interest in the electronic properties of metal hydrides has also increased.

Single-crystalline epitaxial thin films provide an excellent platform for understanding the functionality of metal hydrides and for creating and improving new functionality. For example, epitaxial thin films allow us to observe the intrinsic properties of materials unaffected by grain boundaries [(7)]. Moreover, if thin films are grown in layer-by-layer mode, thickness and flatness can be controlled at the atomic to nano-level [(8,9)]. Furthermore, by selecting an appropriate single-crystal substrate and controlling the orientation, it is possible to change the atomic arrangement at the surface and interface. Therefore, by using epitaxial thin films, material properties can be varied by these detailed material designs. Moreover, epitaxial thin films can be directly used in advanced devices such as light emitting diodes and surface acoustic wave devices, making them attractive from a practical aspect, too. However, the synthesis of epitaxial films of metal hydrides are a relatively new field that began in earnest with the LiH research in 2014 [(9,10,11,12,13,14)]. Therefore, there are many metal hydrides which have never been synthesized as epitaxial thin films.

To promote epitaxial thin film research on hydrides, it is desirable to develop a deposition method that can be widely used for metal hydrides. What is promising from this perspective is the Infrared laser deposition [(15,16)]. This method can synthesize thin films at low energy, and thus it has been used to synthesize thin films of pentacene [(15)] and fullerenes [(16)] with molecular structures that subject to break in high-energy processes of conventional film growth methods such as ultraviolet pulsed laser deposition (PLD) and sputtering. Recently, the infrared laser deposition has also been applied to hydrides with molecular structures called complex hydrides [(17, 18)].

One of the reasons why infrared laser deposition is expected to be an appropriate deposition method for metal hydrides is that this method is less prone to the formation of impurity phases. It is generally known that thin film growth is affected by the energy of the laser heating the raw material. For example, in the ultraviolet PLD method, which uses a powerful ultraviolet laser (Typical photon energy is about 5.0 eV, irradiation energy is about 10 MW cm^{-2}), the extremely active plasma generated when the raw material evaporates can react with the substrate and produce impurities. A typical example would be the LiH film which contains Li_2O formed as a results of the reaction between the film and the MgO substrate during ultraviolet PLD process[(11)]. On the other hand, the infrared laser we use has low

photon energy (1.5 eV at 808 nm) and irradiation energy (~200 W cm^{-2}), so it does not generate plasma and should suppress impurity formation.

Another reason why infrared laser deposition is attractive is that this method can allow us to explore materials rapidly. In this method, an infrared laser heats the target from outside the chamber to deposit thin films. Due to this equipment configuration, we can change film species by simply changing the target, which is usually prepared by simply pressing the commercially available powders.

Though using infrared laser apparently merit metal hydride film growth, we should keep it in mind that use of the low energy can lower hydrogenation ability of the method to form the metal hydrides from metals.

In this study, we work on synthesis of LiH epitaxial films using the hydrogen (H)- radical infrared laser deposition, which reinforces hydrogenation ability of the method. First, we show that the infrared laser deposition suppresses the formation of impurities, but hydrogenation of metallic Li is insufficient without H-radical. Next, we show that the use of H-radical drastically promote hydrogenation of metallic Li and gives LiH epitaxial thin films without residual Li. Then we confirm the fast material exploration capability of the H-radical reactive infrared laser deposition by quickly preparing LiH epitaxial films with five different concentrations of Mg. Finally, we change LiH orientation to show the advanced materials designability of our method.

2. EXPERIMENTAL SECTION

Deposition of LiH thin films was performed by infrared laser deposition or H-radical reactive infrared laser deposition on single-crystal substrates heated to 250 °C in a high vacuum chamber with a back pressure of approximately 1.0 × 10^{-8} Torr (Figure 1). MgO(100) single-crystal substrates (Crystal Base Co., Ltd.) were usually used as a substrate, MgO(110), MgO(111), Al_2O_3(0001), LiF(100), $MgAl_2O_4$(100) (Crystal Base Co., Ltd.) single-crystal substrates were also used for some purposes. These substrates were ultrasonically cleaned with acetone and ethanol before use. Targets were made of LiH powder (Mitsuwa Chemicals Co., Ltd., 97 %) or a mixture of LiH and MgH_2 (FUJIFILM Wako Pure Chemical Co., 99.0+ %), pressed by a uniaxial press at 60 MPa to form pellets with a diameter of 20 mm and thickness of about 1.0 mm. During deposition, these targets were heated by an infrared laser (wavelength 808 nm) (LIMO32-F-400-DL808-EX2024). The substrate-target distance was about 60 mm and the target rotation speed was 60-120 rpm.

H_2 gas with a partial pressure of 1.0 × 10^{-2} Torr was supplied as the reaction gas during infrared laser deposition. In addition, H-radical generated by breaking the H-H bonds of H_2 gas with a high-temperature tungsten filament inside a homemade H-radical generator (H-generator) was supplied as the reaction gas during radical reactive infrared laser deposition [19]. To observe how the growth of the hydride phase changes with the concentration of the generated H-radical, the H_2 gas partial pressure P_{H2} inside the H-generator was set to 1 × 10^{-4}, 1 × 10^{-3}, and 1 × 10^{-2} Torr, and the tungsten filament temperature T_f was changed to 1500 K, 1800 K, and 2000 K [20].

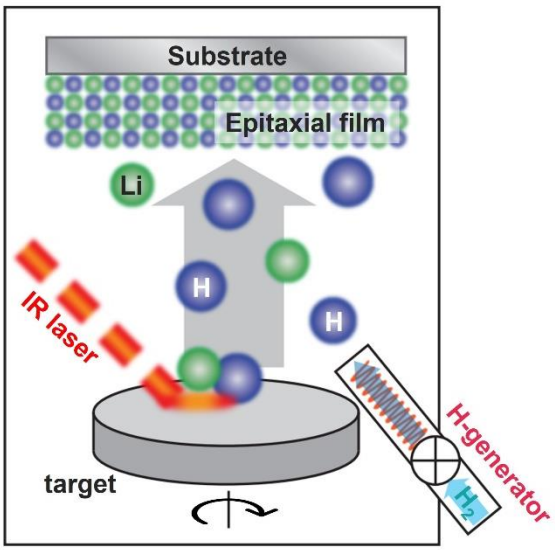

Figure 1. Schematic of LiH epitaxial thin film synthesis by H-radical reactive infrared laser deposition. Metallic Li reacts with hydrogen to grow LiH phase.

The crystal structure of the samples was evaluated by X-ray diffractometer (XRD) (SmartLab, Rigaku and Empyrean 3, Malvern), surface topography by optical microscope (ME-LUX2, KYOWA OPTICAL CO.), scanning electron microscope (SEM) (JSM-7800F, JEOL), and atomic force microscope (AFM) (MultiMode 8, Bruker AXS).

Lithium-ion conductivity was measured by electrochemical impedance method using an impedance meter (SP-150, Biologic) in a vacuum chamber with a back pressure of approximately 1.0 × 10^{-7} Torr. Since hydrides are moisture-sensitive materials, all of the above evaluations were performed in a non-air-exposure environment. A copper film was deposited as a surface protective layer for XRD measurements.

3. RESULTS AND DISCUSSIONS

The LiH thin film without any impurity formation between the substrate and the film was deposited by the infrared laser deposition. Figure 2 shows the XRD $2\theta/\theta$ pattern of the film. The 200-diffraction peak of LiH clearly appears at 2θ = 44.35°, indicating that a 100-oriented LiH film was

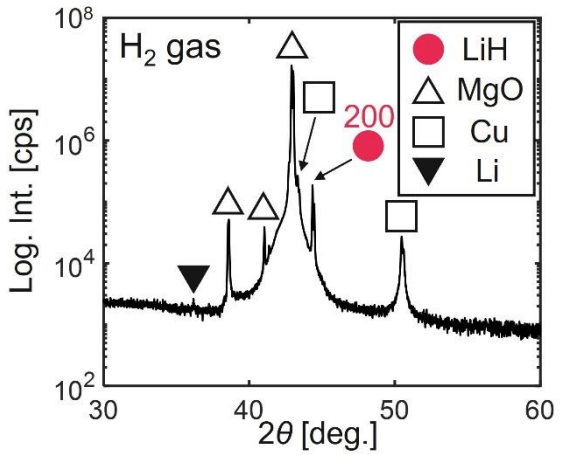

Figure 2. The $2\theta/\theta$ XRD patterns of a LiH film grown at $P_{H2} = 10^{-2}$ Torr, T_f = Room temperature.

obtained. The Li_2O-derived peaks appeared in the UV PLD experiments were not observed. However, a diffraction peak derived from metallic Li was observed at $2\theta = 36.07°$, indicating that the metal remained in the film due to a decrease in hydrogenation ability of the method.

To promote the hydrogenation of the metallic Li, films were then deposited by the H-radical reactive infrared laser deposition. Figure 3 shows microscopic images of thin films synthesized under the H-radical atmosphere generated at different P_{H2} and T_f. The inset shown in the upper right corner of each microscopic image is a photograph of the sample. The film synthesized by the infrared laser deposition (P_{H2} = 1.0 × 10^{-2} Torr, T_f = RT) was almost entirely composed of metallic Li under the microscope (Figure 3a). The electrical resistance of the film measured by a multimeter was about 12.4 kΩ, which is clearly low for insulating LiH with a band gap of 4 eV. Next, the synthesis was carried out with the P_{H2} remaining unchanged and the T_f set to 1500 K to generate H-radical. The size of the island of metallic Li was reduced, suggesting that a part of metallic Li was hydrogenated (Figure 3b). Further increasing the T_f and increasing the amount of H-radical promoted hydrogenation, and at T_f = 1800 K (Figure 3c) and 2000 K (Figure 3d), the metal Li disappeared from the microscopic images. The thin film was almost transparent at these T_f. These results suggest that the reaction between metallic Li and H-radical proceeds as the amount of H-radical is increased, and the percentage of LiH in the film increases. A similar trend was observed when the amount of H-radical was varied by P_{H2}. In both cases of T_f = 1800 K and 2000 K, islands of the metallic Li became smaller as P_{H2} increased from 1×10^{-4} Torr (Figure 3g, 3h) to 1×10^{-3} Torr (Figure 3e, 3f), and the islands disappear completely at $P_{H2} = 1\times10^{-2}$ Torr (Figure 3c, 3d). At the same P_{H2}, the higher the T_f lower the area of the metallic Li islands.

XRD $2\theta/\theta$ measurements and φ-scan measurements of the films grown at $P_{H2} = 1\times10^{-2}$ Torr and T_f = 2000 K showed that a single phase and highly crystalline LiH epitaxial thin film was obtained successfully. There was no Li-derived peak, indicating that hydrogenation has completely progressed. Since only the LiH 200 diffraction peak was a peak attributed to the thin film, the obtained film was found to be a single-phase LiH film. The

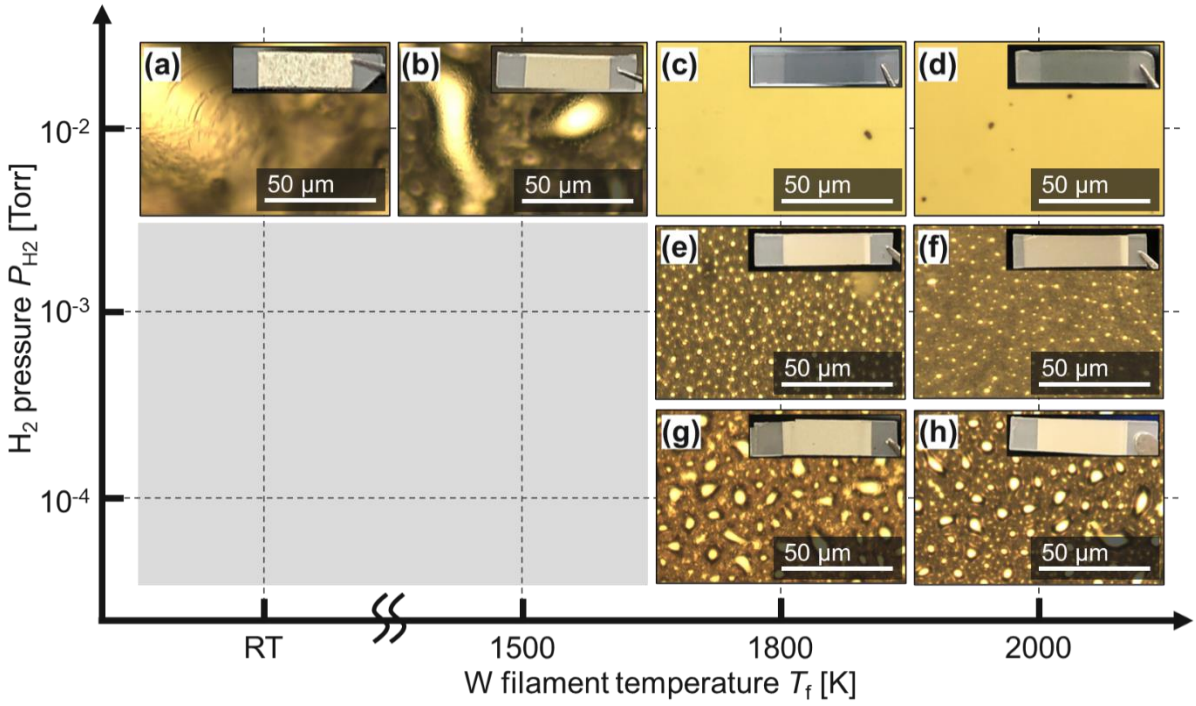

Figure 3. Photographs and optical microscopic images of films synthesized at different H_2 pressure P_{H2} and tungsten filament temperature T_f.

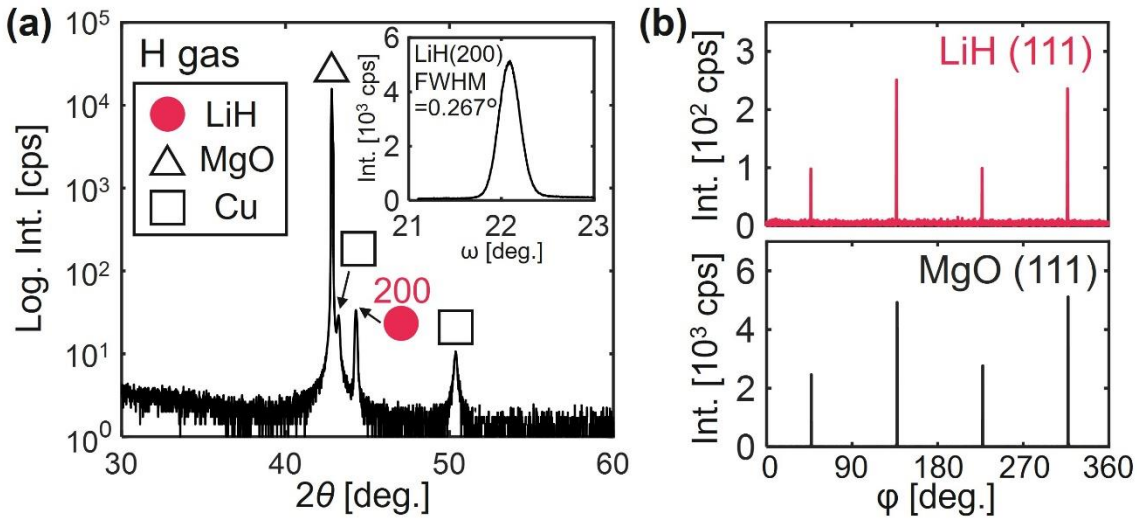

Figure 4. A set of XRD measurements of LiH thin films. (a) The $2\theta/\theta$ XRD patterns grown at $P_{H2} = 10^{-2}$ Torr, $T_f = 2000$ K. The inset shows the XRD rocking curves for LiH 200 plane. (b) The in-plane φ scan pattern of the 200 peak of the thin film and the substrate.

peaks at $2\theta = 42.82°$ originate from the MgO(100) substrate, and the peaks at $2\theta = 43.24°$ and 50.38° originate from the Cu surface protection film. The FWHM value of the XRD rocking curve is 0.267°. This value is about 75 % smaller than that of the LiH epitaxial film fabricated on MgO(100) substrate using the UV PLD (0.36°), suggesting an improvement in crystallinity. Figure 4b shows the φ-scan pattern of the sample, in which 111 reflections of the LiH film and the MgO substrate appear at the same angle every 90°, indicating that the obtained LiH film is an epitaxial film. The epitaxial relationship between this film and the substrate was LiH(010)//MgO(010) in the in-plane direction and LiH(100)//MgO(100) in the out-of-plane direction. The impurity-free 100-oriented LiH epitaxial films were also obtained on LiF (100) and $MgAl_2O_4$ (100) substrates (Figure S1), demonstrating that the films can be deposited on a variety of substrates. The availability of a variety of substrates is an advantage for future material design. For example, it will be possible to synthesize hydride films with different amounts of lattice distortion on substrates with different lattice matching.

SEM and AFM observations show that the quality of LiH epitaxial thin films synthesized by the H-radical reactive infrared laser deposition is very high. Figure 5a shows a cross-sectional SEM image of the LiH epitaxial thin film. The film was densely deposited over the entire surface of the substrate without any noticeable holes. The thickness was almost the same at all positions on the substrate, indicating that the film was grown uniformly. EDS mapping (Figure 5b, 5c) shows that there was no elemental diffusion from the substrate to the film and that a sharp interface was formed. The surface of the films was extremely flat, with an average room mean square roughness R_{rms} of 1.389 nm as determined by analysis of the AFM images (Figure 5d).

The ability of the H-radical reactive infrared laser deposition method to rapidly explore materials was also investigated. Figure 6a shows the XRD $2\theta/\theta$ diffraction patterns of the thin films synthesized using LiH targets containing 0, 0.50, 1.0 and 2.0 at% Mg. (Although the amount of Mg added to the thin films does not always match that of the target, nominally, the compositional formula of the films prepared with a target containing x at% MgH_2 is denoted as $Li_{1-x/100}Mg_{x/100}H$.) No diffraction peaks from Mg or MgH_2 were observed in these films. And the peak corresponding to LiH 200 diffraction shifted to a lower angle as the Mg content of the target increased. The lattice constant calculated from the diffraction angle of this peak (Figure 6b) increased in proportion to the Mg concentration in the target up to $x = 2$, suggesting that the amount of Li substitution by Mg with a larger ionic radius increased. These results demonstrate that the composition of thin film samples can be systematically changed simply by changing the target composition.

The $Li_{1-x/100}Mg_{x/100}H$ films exhibit interesting physical properties. Figure 6c shows the Nyquist plots obtained by impedance measurements on LiH and $Li_{0.98}Mg_{0.02}H$ epitaxial films heated to 393 K. Both films show a semicircle with little distortion, and the capacitance components determined from the semicircle analysis are 1.23×10^{-10} F for LiH and 1.18×10^{-10} F for $Li_{0.98}Mg_{0.02}H$, respectively, which correspond to the Li ion conduction in the crystal grains. When Au is used as a blocking electrode, a straight line appears at low frequencies. While Li is used as a non-blocking electrode, the

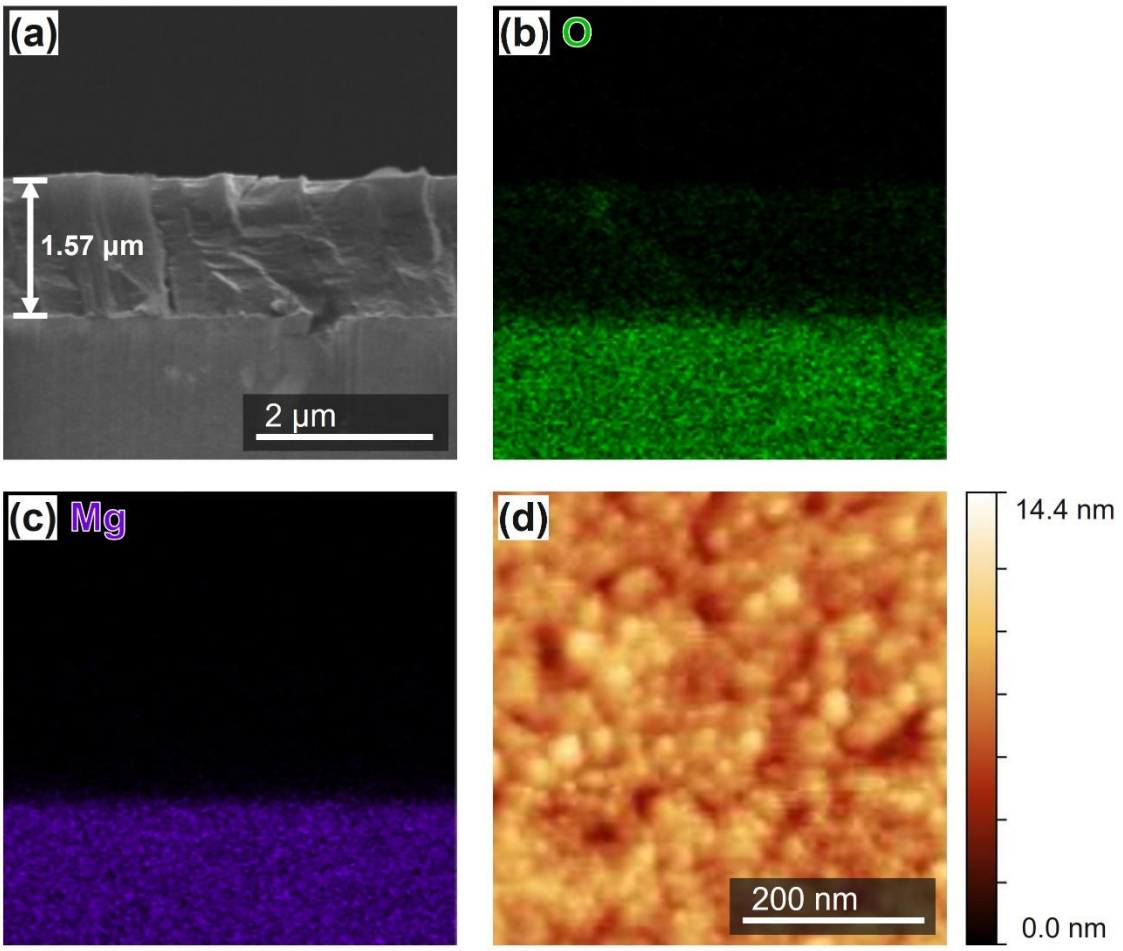

Figure 5. (a), A cross-sectional SEM image and (b)-(c) EDS mappings of a LiH epitaxial thin film grown on a MgO substrate at T_f = 2000 K. EDS mappings are for (b) O, and (c) Mg elements. (d) An AFM image grown at T_f = 2000 K.

line disappears. These observation confirmed the Li ion conductivity of the film [21]. Figure 6d is an Arrhenius plot showing the temperature dependence of the Li ion conductivity determined from the analysis of the Nyquist plot. Mg doping increases the Li ion conductivity of the LiH film, and at 323 K, the conductivity of the $Li_{0.98}Mg_{0.02}H$ film was 4.5 × 10^{-8} S cm-1, about 20 times higher than the conductivity of the LiH film, 1.9 × 10^{-9} S cm^{-1}. One possible reason for this is the occurrence of Li deficiency due to the substitution of monovalent Li sites by divalent Mg. The lower activation energy for Li conduction (59.5 kJ mol^{-1} → 19.8 kJ mol^{-1}) may also have contributed to the increased conductivity.

The Mg substitution for LiH observed in this study was likely caused by the epitaxial thin film. In general, hydrides have smaller formation Gibbs energy than nitrides or oxides (LiH: -68.37 kJ/mol, Li_3N: -128.4 kJ/mol, Li_2O: -561.2 kJ/mol), which makes their structures unstable and substitution unlikely to occur. In fact, in the powder sample synthesized in this study, in which Mg was added to LiH, Mg substitution did occur, and unlike the epitaxial thin film, increase in Li ion conductivity was not observed (Figure S2). The Mg substitution occurred in the epitaxial thin film, probably because the strong interaction between the substrate and the thin film stabilizes the structure [22]. The lattice constants of the films fabricated in this study are in good agreement with previously reported values [23] (Figure S3), suggesting that stress did not contribute to the substitution of lattice distortion.

In this study, we also deposited films on MgO(110), MgO(111), and Al_2O_3(0001) substrates. Then, 110-oriented LiH epitaxial films are obtained on MgO(110), while 111-oriented ones are obtained on MgO(111) and Al_2O_3(0001) substrates (Figure S4). The latter was surprising because, in the previous study done by Oguchi et. al., they could obtain only polycrystalline films mixed with $LiAlO_2$ on Al_2O_3(0001) substrates by vapor-liquid-solid method. Therefore, this result not only reinforces our hypothesis that the H-radical reactive infrared laser deposition is a suitable technique for obtaining single-phase films by suppressing substrate-film reactions, but also suggests that this method can be used to grow the uniaxially oriented epitaxial films.

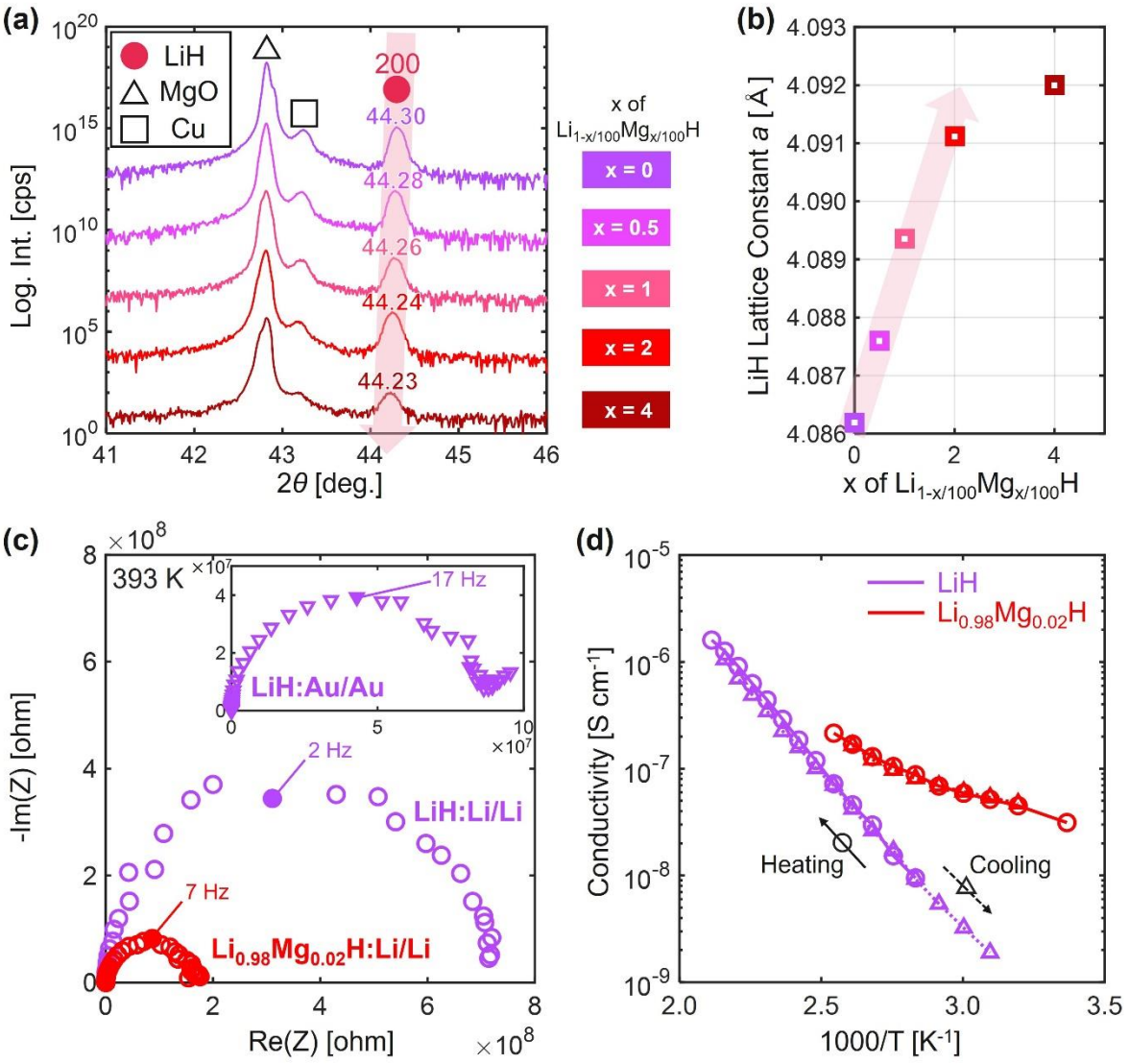

Figure 6. (a) The $2\theta/\theta$ XRD measurements of Mg-doped LiH epitaxial thin films. Films doped with 0 at% (violet), 0.50 at% (red-violet), 1.0 at% (pink), 2.0 at% (red) and 4.0 at% (brown). The ratio here refers to the ratio of MgH_2 mixed in the LiH targets. (b) Mg concentration dependence of lattice constant of Mg-doped LiH epitaxial thin films. (c) Nyquist plots of $Li_{(1-x)}Mg_xH$ epitaxial films obtained at 120 ˚C. (d) Temperature dependence of Li-ion conductivity of LiH(violet) and $Li_{0.98}Mg_{0.02}H$ films. Samples were first heated (323 K → 473 K) and then cooled (473 K → 323 K).

As shown in the above studies, the H-radical reactive infrared laser deposition is an excellent synthesis method for hydride epitaxial thin films. On the other hand, this method has a drawback that H-radical may roughen the substrate surface and lower the crystallinity of the films. Figure 7 shows XRD rocking curves of two types of films obtained with two different T_f. For T_f = 1500 K and 2000 K, the FWHMs are 0.17° and 0.26°, respectively, indicating that the crystallinity of the films decreases as the H-radical concentration increases. To investigate the cause of this problem, the MgO(100) substrate surface was observed in situ by reflection high energy electron diffraction (RHEED) while irradiated with H-radical (T_f = 2000 K). Figure 8 shows the obtained RHEED images. The RHEED image obtained at t = 0 min (Figure 8a), immediately after the start of H-radical irradiation, shows a streak pattern indicating atomic-level flatness. However, the streak intensity began to decrease as early as t = 5 min (Figure 8b) and changed to a spot-like pattern at t = 30 min (Figure 8c). These changes suggest a decrease in the flatness of the substrate surface [24]. In fact, AFM observation confirmed the flatness degradation. Figure 8d and 8e show AFM images of MgO(100) substrate surfaces irradiated with H-radical for 0 min and 15 min, respectively. The R_{rms} of the substrate surface calculated by analyzing these images was 0.4172 nm at t = 0 min, but 2.863 nm at t = 15 min. In the future, if we need to improve crystallinity of the films, it will be necessary to take measures such as protection of the substrate surface.

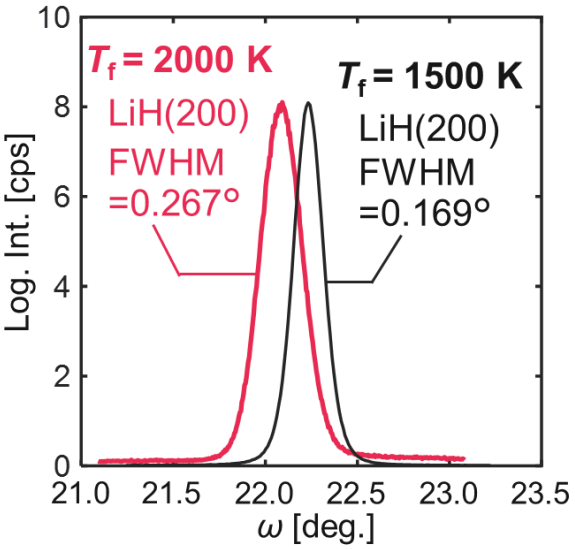

Figure 7. XRD rocking curves for 200 plane of LiH epitaxial thin films. The $2\theta/\theta$ XRD patterns grown at P_{H2} = 10^{-2} Torr, T_f = 1500 K(black) and 2000 K(red).

4. CONCLUTION

In this study, we established a H-radical reactive infrared laser deposition as an effective method for epitaxial thin film synthesis of metal hydrides. We have demonstrated that a low energy infrared laser can suppress substrate-film interface reactions, while a highly active H-radical can strongly promote metal hydrogenation. The ability the method to suppress reactions at the substrate-film interface has also made it possible to use a wide variety of substrates. We also fabricated LiH films with five different amounts of Mg substitution and demonstrated that this method is suitable for fast materials exploration. The previously unreported Mg substitution occurred in these LiH films indicate that the epitaxial thin films are possible platform to conduct unprecedented elemental substitution studies on metal hydrides. The H-radical reactive infrared laser deposition will open up new way of material design of metals hydrides, such as elemental substitution, orientation control, and lattice distortion, which will lead to the control of optical, electrical, mechanical properties and so on that have been impossible in the conventional hydrides research.

ASSOCIATED CONTENT

Supporting Information

$2\theta/\theta$ diffraction patterns and φ scan patterns of LiH thin films deposited on five different substrates (LiF(100), $MgAl_2O_4$(100), MgO(110), MgO(111) Al_2O_3(0001)) with different orientations and compositions instead of MgO(100) substrate; Comparison of optical microscopic images of $Li_{(1-x)}Mg_xH$ polycrystalline films, epitaxial films, and powders; XRD diffraction patterns for symmetric 100 plane and asymmetric 110 plane of a $Li_{0.96}Mg_{0.04}H$ epitaxial thin film.

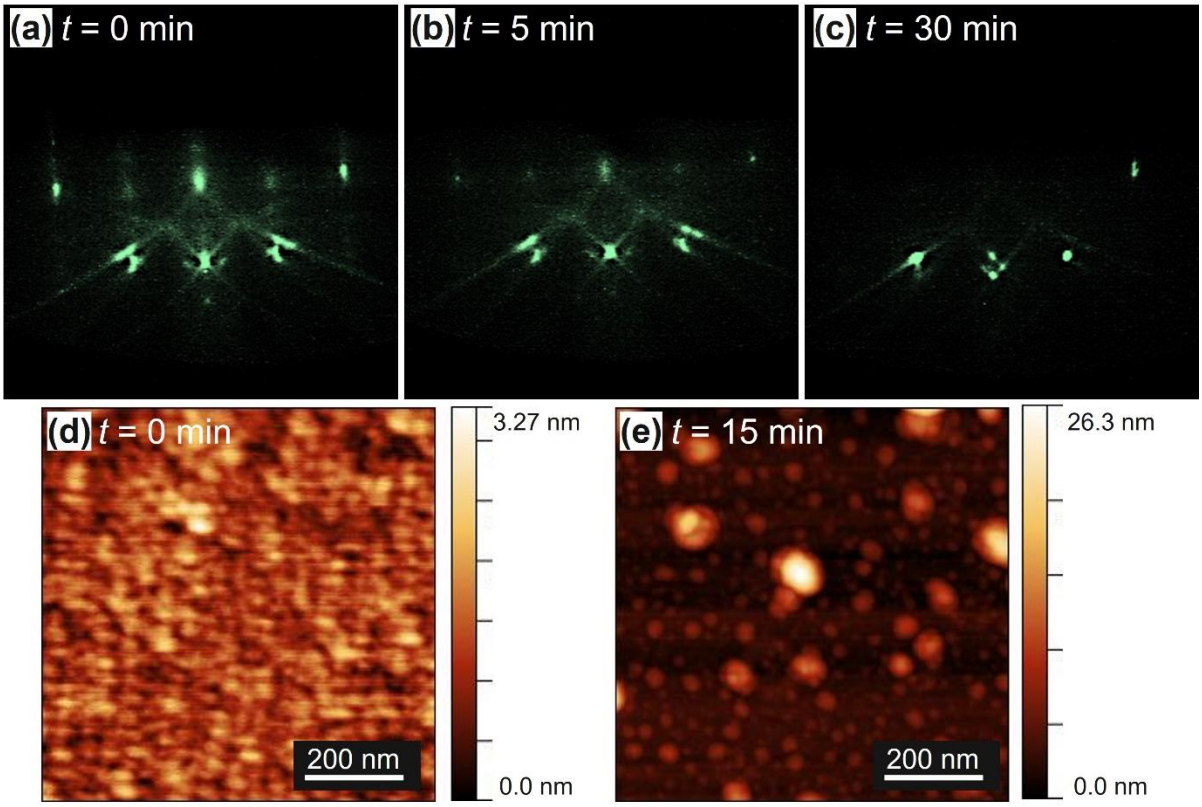

Figure 8. RHEED patterns of MgO substrates irradiated by H-radical for (a) 0 min, (b) 5 min, and (c) 30 min. (d, e) AFM images of MgO substrates irradiated by H-radical generated at T_f = 2000 K for (d) 0 min and (e) 15 min.

AUTHOR INFORMATION

Corresponding Author

Hiroyuki Oguchi − *Department of Applied Chemistry, Graduate School of Engineering and Science, Shibaura Institute of Technology, 3-7-5 Toyosu, Koto-ku, Tokyo, Japan*
E-mail: h-oguchi@shibaura-it.ac.jp

Authors

Kota Munefusa − *Department of Applied Chemistry, Graduate School of Engineering and Science, Shibaura Institute of Technology, 3-7-5 Toyosu, Koto-ku, Tokyo, Japan*
E-mail: mc22036@shibaura-it.ac.jp

Erika Fukushi − *Department of Applied Chemistry, Graduate School of Engineering and Science, Shibaura Institute of Technology, 3-7-5 Toyosu, Koto-ku, Tokyo, Japan*
E-mail: mc22029@shibaura-it.ac.jp

Junya Tanaka − *Department of Applied Chemistry, Graduate School of Engineering and Science, Shibaura Institute of Technology, 3-7-5 Toyosu, Koto-ku, Tokyo, Japan*
E-mail: ad20049@shibaura-it.ac.jp

Takayuki Harada − *National Institute for Materials Science, Research Center for Materials Nanoarchitectonics (MANA), 1-1 Namiki, Tsukuba, Ibaraki, Japan*
E-mail: HARADA.Takayuki@nims.go.jp

Author Contributions

K.M. and H.O. planned the experiments; K.M. performed synthesis, evaluation, and data analysis; E.F. and J.T. assisted with synthesis; and T.H. assisted with XRD measurements. All authors discussed the results and commented on the manuscript.

ACKNOWLEDGMENTS

This work was supported by Grant-in-Aid for Challenging Exploratory Research (7K19 K22225), the S-SPIRE project at Shibaura Institute of Technology (23017), and the NIMS Collaboration Center Promotion Program (2022-87) (2023-024). We thank Associate Professor Masaki Nakano of the Quantum Phase Electronics Research Center, Department of Physics and Engineering, Graduate School of Engineering, the University of Tokyo for his assistance with XRD measurements. Dr. Kyosuke Matsushita and Dr. Makiko Oshida of the Battery Research Platform, National Institute for Materials Science (NIMS) for their assistance with AFM and SEM measurements, and Dr. Masatomo Sumiya of the National Institute for Materials Science (NIMS) for development of a H-radical generator, and Professor Mikk Lippmaa for his assistance with AFM measurements.

REFERENCES

(1) Mohtadi, R.; Orimo, S. The renaissance of hydrides as energy materials. *Nat. Rev. Mater*. **2016**, *2*, 16091.

(2) Orimo, S.; Nakamori, Y.; Eliseo, J. R.; Züttel, A.; Jensen, C. M. Complex Hydrides for Hydrogen Storage. *Chem. Rev.* **2007**, *107*, 10, 4111-4132.

(3) Verbraeken, M. C.; Cheung. C; Suard, E; Irvine, J. T. S. High H^- ionic conductivity in barium hydride. *Nat. Mater.* **2005**, *14*, 95-100.

(4) Griessen, R.; Huiberts, J. N.; Kremers, M.; van Gogh, A. T. M.; Koeman, N. J.; Dekker, J. P.; Notten, P. H. L. Yttrium and lanthanum hydride films with switchable optical properties. *J. Alloys Compd.* **1997**, *253-254*, 20, 44-50.

(5) Somayazulu, M.; Ahart, M.; Mishra, A. K.; Geballe, Z. M.; Baldini, M.; Meng, Y.; Struzhkin, V. V.; Hemley, R. J. Evidence for Superconductivity above 260 K in Lanthanum Superhydride at Megabar Pressures. *Phys. Rev. Lett.* **2019**, *122*, 027001.

(6) Drozdov, A. P.; Eremets, M. I.; Troyan, I. A.; Ksenofontov, V.; Shylin, S. I. Conventional superconductivity at 203 kelvin at high pressures in the sulfur hydride system. *Nature* **2015**, *525*, 73.

(7) Fukushi, E.; Mori, F.; Munefusa, K.; Harada, T.; Oguchi, H. Epitaxial Thin Film Growth of Perovskite Hydrides MLiH$_3$ (M : Sr, Ba) for The Study of Intrinsic Hydride-Ion Conduction. *ACS Appl. Energy Mater.* **2023**, Accepted.

(8) Kumigashira, H.; Horiba, K.; Ohguchi, H.; Kobayashi, D.; Oshima, M.; Nakagawa N.; Ohnishi, T.; Lippmaa, M.; Ono, K.; Kawasaki. M.; Koinuma, H. In situ photoemission spectroscopic study on $La_{1-x}Sr_xMnO_3$ thin films grown by combinatorial laser-MBE. *J. electron spectros. relat. phenomena* **2004**, *136*, 1-2, 31-36.

(9) Yoshimatsu, K.; Suzuki, T.; Tsuchimine, N.; Horiba, K.; Kumigashira, H.; Oshima, T.; Ohtomo, A. Direct growth of metallic TiH_2 thin films by pulsed laser deposition. *Appl. Phys. Express* **2005**, *8*, 035801.

(10) Oguchi, H.; Ikeshoji, T.; Ohsawa, T.; Shiraki, S.; Kuwano, H.; Orimo, S.; Hitosugi, T Epitaxial thin film growth of LiH using a liquid-Li atomic template, *Appl. Phys. Lett.* **2014**, *105*, 211601.

(11) Oguchi, H.; Isobe, S.; Kuwano, H.; Shiraki, S.; Orimo, S.; Hitosugi, T. Pulsed laser deposition of air-sensitive hydride epitaxial thin films: LiH. *APL Mater.* **2015**, *3*, 096106.

(12) Shimizu, R.; Sasahara, Y.; Oguchi, H.; Yamamoto, K.; Sugiyama, I.; Shiraki, S., Orimo, S.; Hitosugi, T. Fabrication of atomically abrupt interfaces of single-phase TiH_2 and Al_2O_3. *APL Mater.* **2017**, *5*, 086102.

(13) Shimizu, R.; Kakinokizono, T.; Gu, I.; Hitosugi, T. Epitaxial Growth of Single-Phase

Magnesium Dihydride Thin Films. *Inorg. Chem.* **2019**, *58*, 15354-15358.
(14) Komatsu, Y.; Shimizu, R.; Wilde, M.; Kobayashi, S.; Sasahara, Y.; Nishio, K.; Shigematsu, K.; Ohtomo, A.; Fukutani, K.; Hitosugi, T. Epitaxial Thin Film Growth of Europium Dihydride. *Cryst. Growth Des.* **2020**, *20*, 5903-5907.
(15) Yaginuma, S.; Yamaguchi, J.; Haemori, M.; Itaka, K.; Matsumoto, Y.; Kondo, M.; Koinuma, H. Continuous wave infrared laser deposition of organic thin films. *Conf. Ser.* **2007**, *59*, 520-525.
(16) Yaginuma, S.; Itaka, K.; Haemori, M.; Katayama, M.; Ueno, K.; Ohnishi, T.; Lippmaa, M.; Matsumoto, Y.; Koinuma, H. Molecular Layer-by-Layer Growth of C_{60} Thin Films by Continuous-Wave Infrared Laser Deposition. *Appl. Phys. Express* **2008**, *1*, 015005.
(17) Oguchi, H.; Kim, S.; Maruyama, S.; Horisawa, Y.; Takagi, S.; Sato, T.; Shimizu, R.; Matsumoto, Y.; Hitosugi, T.; Orimo, S. Epitaxial Film Growth of $LiBH_4$ via Molecular Unit Evaporation. *ACS Appl. Electron. Mater.* **2019**, *1*, 1792-1796.
(18) Nakayama, R.; Kawaguchi, Y.; Shimizu, R.; Nishio, K.; Oguchi, H.; Kim, S.; Orimo, S.; Hitosugi, T. Fabrication and Growth Orientation Control of $NaBH_4$ Epitaxial Thin Films Using Infrared Pulsed-Laser Deposition. *Cryst. Growth Des.* **2022**, *22*, 11, 6616-6621.
(19) Dahmani, F. Z.; Okamoto, Y.; Tsutsumi, D.; Ishigaki, T.; Koinuma, H.; Hamzaoui, S.; Flazi, S.; Sumiya, M. Density evaluation of remotely-supplied hydrogen radicals produced via tungsten filament method for $SiCl_4$ reduction. *Jpn. J. Appl. Phys.* **2018**, *57*, 5, 051301.
(20) Okamoto, Y.; Sumiya, M.; Nakamura, Y.; Suzuki, Y. Effective silicon production from $SiCl_4$ source using hydrogen radicals generated and transported at atmospheric pressure. *Sci. Tech. Adv. Mater.* **2020**, *21*, 1, 482-491.
(21) Pretzel, F. E.; Rupert, G. N.; Mader, C.L.; Storms, E. K.; Gritton, G. V.; Rushing, C. C. Properties of lithium hydride I. Single crystals. *J. Phys. Chem. Solids* **1960**, *16*, 1-2, 10-20.
(22) Nishii, J.; Ohtomo, A.; Ikeda, M.; Yamada, Y.; Ohtani, K.; Ohno, H.; Kawasaki, M. High-throughput synthesis and characterization of $Mg_{1-x}Ca_xO$ films as a lattice and valence-matched gate dielectric for ZnO based field effect transistors. *Appl. Surf. Sci.* **2006**, *252*, 7, 2507-2511.
(23) Tyutyunnik, O. I.; Tyutyunnik, V. I.; Shulgin, B. V.; Oparin, D. V.; Pilipenko, G. I.; Gavrilov, F. F. Lithium hydride single crystal growth by bridgman-stockbarger method using ultrasound. *J. Cryst. Growth* **1984**, *68*, 3, 741-746.
(24) Gallinat, C. S.; Koblmüller, G.; Wu, F.; Speck, J. S. Evaluation of threading dislocation densities in In- and N-face InN. *J. Appl. Phys.* **2010**, *107*, 053517.